Novel Adaptive Recurrent Chebyshev Neural Network Control for PM Synchronous Motor Servo-Drive Electric Scooter

Chih-Hong Lin

Department of Electrical Engineering, National United University, Miaoli 36003, Taiwan
E-mail:jhlin@nuu.edu.tw

Abstract: Because of unknown nonlinearity and time-varying characteristics of electric scooter driven by permanent magnet synchronous motor (PMSM), its accurate dynamic model is difficult to establish for the design of the linear controller in whole system. In order to conquer this difficulty and raise robustness, an adaptive recurrent Chebyshev neural network (NN) control system is proposed to control for a PMSM servo-drive electric scooter under external torque disturbance in this study. The adaptive recurrent Chebyshev NN control system consists of a recurrent Chebyshev NN control and a compensated control with estimation law. In addition, the online parameters tuning methodology of the recurrent Chebyshev NN and the estimation law of the compensated controller can be derived by using the Lyapunov stability theorem. Finally, comparative studies are demonstrated by experimental results in order to show the effectiveness of the proposed control scheme.

Keywords: Permanent Magnet Synchronous Motor, Chebyshev Neural Network, Lyapunov stability.

1. INTRODUCTION

In recent years, for the purpose of reducing air pollution and enhancing environmental protection, quite a few countries require their automotive industries to develop electric vehicles in place of gasoline-powered automobiles gradually. Here we put our attention on the development and research of electric scooters since scooters are much more widespread than automobiles for individual transportation in Asia. Owing to demand of high power density and high efficiency, the selections of AC motor drive system are very important for the purpose of electric scooter driven by AC motor. Comparing permanent magnet synchronous motors (PMSMs) with other AC motors, PMSMs have many advantages, such as high power density, high efficiency, high robustness, etc. Therefore they have been widely used in many applications of mechatronics (Leonhard, 1996; Lin, 1997; Novotny and Lipo, 1996).

Artificial neural networks (NNs) have emerged as a powerful learning technique to perform complex tasks in highly nonlinear dynamic systems and controls (Ciliz, 2005; Grino *et al.,* 2000; Haykin, 1994; Patino *et al.,* 2002; Sastry *et al.,* 1994; Sefriti *et al.,* 2012; Sun *et al.,* 2000; Sun *et al.,* 2011). Some of the prime advantages of using NN are: their ability to learn based on optimization of an appropriate error function and their excellent performance for approximation of nonlinear functions. There are different paradigms of NNs proposed by different researchers for the task of system identification and control (Ciliz, 2005; Grino *et al.,* 2000; Patino *et al.,* 2002; Sastry *et al.,* 1994; Sefriti *et al.,* 2012; Sun *et al.,* 2000; Sun *et al.,* 2011). The models obtained with this approach are in state-space and work quite effectively in continuous-time domain. Presently, most of the NN-based system identification and control techniques are based on multilayer feedforward NNs or more efficient variation of this algorithm (Ciliz, 2005; Grino *et al.,* 2000; Patino *et al.,* 2002; Sefriti *et al.,* 2012; Sun *et al.,* 2000; Sun *et al.,* 2011). This is due to the fact that these networks are robust and effective in modeling and control of complex dynamic plants.

Pattern classification using Chebyshev NN was first introduced in (Namatame and Ueda, 1992). A Chebyshev polynomial-based unified model NN for static function approximation was developed in (Lee and Jeng, 1998). It is based on a functional link NN with Chebyshev polynomial expansion in which recursive least square learning algorithm is used. It is pointed out that this network has universal approximation capability and has faster convergence than the multilayer feedforward NN. One of the solutions for the problem of slow convergence of multilayer feedforward NN is to use some efficient learning algorithm instead of BP algorithm. In this direction, the scaled complex conjugate gradient algorithm as proposed by (Moller, 1993) is of great importance. This algorithm chooses the search direction and the step size using information from a second order Taylor expansion of the error function. Some of the other proposals on higher order conjugate gradient algorithms can be found in (Battiti, 1992; Charalambous, 1992; Hagan and Menhaj, 1994). For data classification and function interpolation problems a multilayer feedforward NN trained by conjugate gradient algorithm has been developed in (Madyastha and Aazhang, 1994).

The recurrent NN has received increasing attention due to its structural advantage in the modelling of the nonlinear system and dynamic control of the system (Brdys and Kulawski, 1999;

Chow and Fang, 1998; Haykin, 1994; Li *et al.,* 2005; Lu and Tsai, 2008; Payam *et al.,* 2011). These networks are capable of effective identification and control of complex process dynamics, but with the expense of large computational complexity. However, in the complicated nonlinear dynamic system such as PMSM servo-drive electric scooter system, the flux linkage and external force interference is always an important factor. Hence, if each neuron in the recurrent neural networks is considered as a state in the nonlinear dynamic systems, the self-connection feedback type is unable to approximate the dynamic systems efficiently. In order to improve the ability of identifying high-order systems, the recurrent Chebyshev NN has been proposed in this study. It has more advantages than the Chebyshev NN, such as better performance, higher accuracy, dynamic robustness, and fast transient performance.

Owing to real plants with highly nonlinear dynamics, e.g., electric scooter (Lin *et al.,* 2010; Lin and Lin, 2012, 2013; Lin, 2014) PMSM servo-drive electric scooter controlled by an adaptive recurrent Chebyshev NN control system is developed to enhance control performance in the convergent speed of the network and reduce computational complexity in this paper. In (Lin and Lin, 2012), the experimental results of control performance in the hybrid RFNN control system using rotor flux estimator were only implemented at two cases, i.e., 1200 rpm and 2400 rpm cases without adding and shedding load. In (Lin, 2014), the comparative studies of control performances for the hybrid RFNN control system and the hybrid RWNN control system using rotor flux estimator were implemented at two cases, i.e., 1200 rpm case and 2400 rpm case. The speed and current tracking responses of the hybrid RWNN control system using rotor flux estimator have better performances than the hybrid RFNN control system from experimental results. Furthermore, the hybrid modified Elman NN control system was proposed by (Lin, 2013), in order to enhance nonlinear approximation capacity of RNN. In (Lin, 2013), the comparative studies of control performances for the PI control system and the hybrid modified Elman NN control system were implemented at three cases, at four cases, i.e., 1200 rpm case, 2400 rpm case, under external load torque 2 Nm and with adding load and shedding load at 2400 rpm case under external load torque 4 Nm and with adding load and shedding load at 2400 rpm are shown in experimental results. The tracking responses of speed and current of the hybrid modified Elman NN control system have better performances than the PI control system from experimental results. However, the used recurrent NNs have the more complex network structures and activation functions in the middle layer, i.e. Gaussian wavelet function and sigmoid function. Thus, in the above control methods have the slower convergence speed and higher computation complexity. In order to speedup convergence and reduce computational complexity, the adaptive recurrent Chebyshev NN control system with simpler network structure and activation function is developed for controlling the PMSM servo-drive electric scooter in this paper. The adaptive recurrent Chebyshev NN control system, which is composed of a recurrent Chebyshev NN control and a compensated control with estimation law, is applied to PMSM servo-drive electric scooter system. The adaptive recurrent Chebyshev NN control system has fast convergence ability and good generalization capability. In addition, the online parameter tuning methodology of the recurrent Chebyshev NN and the estimation law of the compensated controller can be derived according to Lyapunov stability theorem. The control method, which is not dependent upon the predetermined characteristics of the system owing to the online learning ability being able to capture the system's nonlinear and time-varying behaviors, can adapt to any change in the system characteristics, Finally, the control performance of the proposed adaptive recurrent Chebyshev NN control system is verified by experimental results.

The structure of the paper is as follows. The configuration of PMSG servo-drive electric scooter system is described in Section 2. The design of adaptive recurrent Chebyshev NN control system for PMSG servo-drive electric scooter system is presented in Section 3. Comparative studies are illustrated by experimental results in order to show the effectiveness of the proposed control scheme in Section 4. Some conclusions are given in Section 5.

2. CONFIGURATION OF PMSM SERVO- DRIVE ELECTRIC SCOOTER SYSTEM

The d-axis and q-axis voltage equations of the PMSM servo-drive electric scooter in the rotating reference frame can be described as follows (Leonhard, 1996; Lin, 1997; Novotny and Lipo, 1996):

$$v_{qr} = R_r i_{qr} + L_{qr}\dot{i}_{qr} + P_r\omega_c(L_{dr}\dot{i}_{dr} + \lambda_{fd})/2 \tag{1}$$

$$v_{dr} = R_r i_{dr} + L_{dr}\dot{i}_{dr} - P_r\omega_c L_{qr}\dot{i}_{qr}/2 \tag{2}$$

in which v_{qr} and v_{dr} are the d-axis and q-axis voltages, i_{qr} and i_{dr} are the d-axis and q-axis currents, L_{qr} and L_{dr} are the d-axis and q-axis inductances, λ_{fd} is the d-axis permanent magnet flux linkage, R_r is the stator resistance, ω_c is the rotor speed. The electromagnetic torque T_e of a PMSM servo-drive electric scooter can be described as

$$T_e = 3P_r[\lambda_{fd}i_{qr} + (L_{dr} - L_{qr})i_{dr}i_{qr}]/4 \tag{3}$$

Then the dynamic equation of PMSM can be represented

$$J_r\dot{\omega}_c + B_r\omega_c + T_l = T_e \tag{4}$$

in which P_r is the number of poles, T_l is the external load disturbance, e.g. electric scooter, B_r represents the total viscous frictional coefficient and J_r is the total moment of inertia. Due to $L_{dr} = L_{qr}$ for a surface-mounted PMSM, the second term of (3) is zero. Moreover, λ_{fd} is a constant for surface-mounted PMSM. The rotor flux is produced in the d-axis only, while the current vector is generated in the q-axis for the field-oriented control When the d-axis rotor flux is a constant and torque angle is $\pi/2$ (Lin, 1997; Novotny and

Lipo, 1996), the maximum torque per ampere can be reached for the field-oriented control.

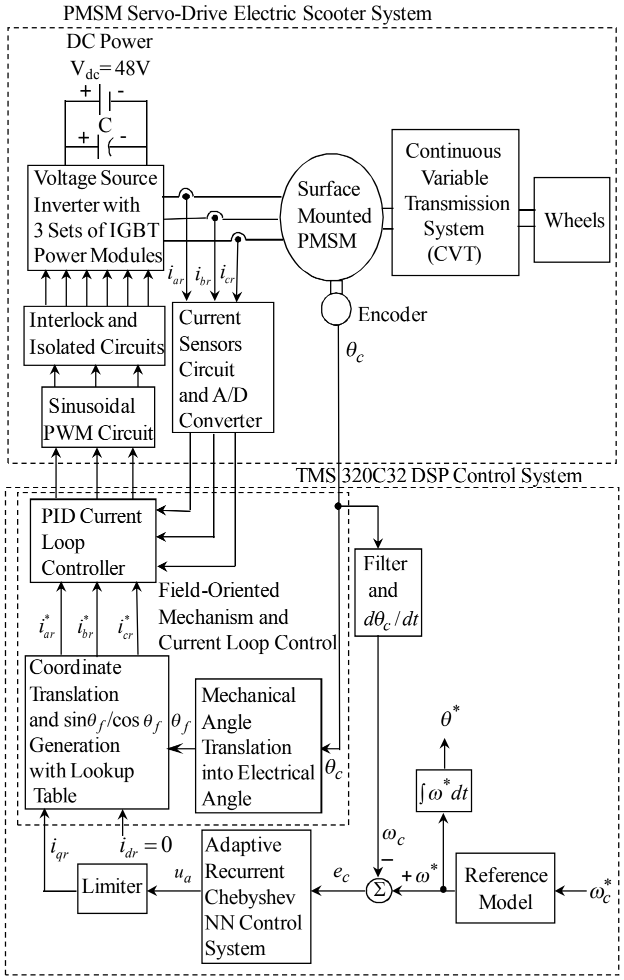

Fig. 1. Block diagram of a PMSM servo-drive electric scooter system.

The electromagnetic torque T_e is linearly proportional to the q-axis current i_{qr}, which is determined by closed-loop control. The PMSM servo-drive system with the implementation of field-oriented control can be reduced as

$$T_e = k_r i_{qr} \tag{5}$$

in which $k_r = 3P_r\lambda_{fd}/4$ is the torque constant. A block diagram of whole system for a PMSM servo-drive electric scooter shown in Fig. 1 can be indicated as follows: a field orientation institution, a proportional integral derivative (PID) current control loop, a sinusoidal pulse width modulation (PWM) control circuit, an interlock circuit and an isolated circuit, a voltage source inverter with 3 sets of insulated gate bipolar transistor (IGBT) power modules and a speed control loop. The PID current controller is the current loop tracking controller. In order to attain good dynamic response, all gains for a PID current controller are listed as follows: $k_{pc}=8$, $k_{ic}=2.5$ and $k_{dc}=0.5$. The field orientation institution makes up coordinate transformation, $\sin\theta_f/\cos\theta_f$ generation and lookup table generation. The TMS320C32 DSP control system is used to implement a field orientation institution, a current control and a speed control. The PMSM servo-drive electric scooter is manipulated at load disturbance torque with nonlinear uncertainty.

3. DESIGN OF ADAPTIVE RECURRENT CHEBYSHEV NN CONTROL SYSTEM

Due to nonlinear uncertainties of the electric scooter such as nonlinear friction force of the transmission belt and clutch, these will lead to degenerate tracking responses in command current and speed of the PMSM servo-drive electric scooter. The variation of rotor inertia and friction of PMSM servo-drive electric scooter cause nonlinear uncertainties. These uncertainties are difficult to establish exact models. Therefore, for convenient design of adaptive recurrent Chebyshev NN control system, the dynamic equation of the PMSM servo-drive electric scooter from (4) can be rewritten as

$$\begin{aligned}\dot{\omega}_c &= -B_r\omega_c/J_r - T_l/J_r + k_r i_{qr}/J_r \\ &= A_a\omega_c + C_aT_l + B_a u_a \end{aligned} \tag{6}$$

in which $u_a = i_{qr}$ is the q-axis command current of the PMSM. $A_a = -B_r/J_r$, $B_a = k_r/J_r$ and $C_a = -1/J_r$ are three known constants.

When the uncertainties including variation of system parameters and external force disturbances occur, the parameters are assumed to be bounded, i.e., $|A_a\omega_c| \le D_1(\omega_c)$, $|C_aT_l| \le D_2$ and $B_a \le D_3$, where $D_1(\omega_c)$ is a known continuous function, D_2 and D_3 are two bounded constants. Then, the tracking error can be defined as

$$e_c = \omega^* - \omega_c \tag{7}$$

where ω^* represents the desired command rotor speed, e_c is the tracking error between the desired rotor speed and rotor speed. If all parameters of the PMSM servo-drive system including external load disturbance are well known, the ideal control law can be designed as

$$u_a^* = [\dot{\omega}^* + k_1e_c - A_a\omega_c - C_aT_l]/B_a \tag{8}$$

in which $k_1 > 0$ is a constant. Replacing (8) of (6), the error dynamic equation can be obtained

$$\dot{e}_c + k_1e_c = 0 \tag{9}$$

If the dynamic error is imposed by (9) and take into account (6) and (7), then ideal control is of the form (8). The system state can track the desired trajectory gradually if $e_c(t) \to 0$ as $t \to \infty$ in (9). However, the adaptive recurrent Chebyshev NN control system is proposed to control PMSM servo-drive electric scooter under uncertainty perturbation. The configuration of the proposed adaptive recurrent Chebyshev NN control system is described in Fig. 2.

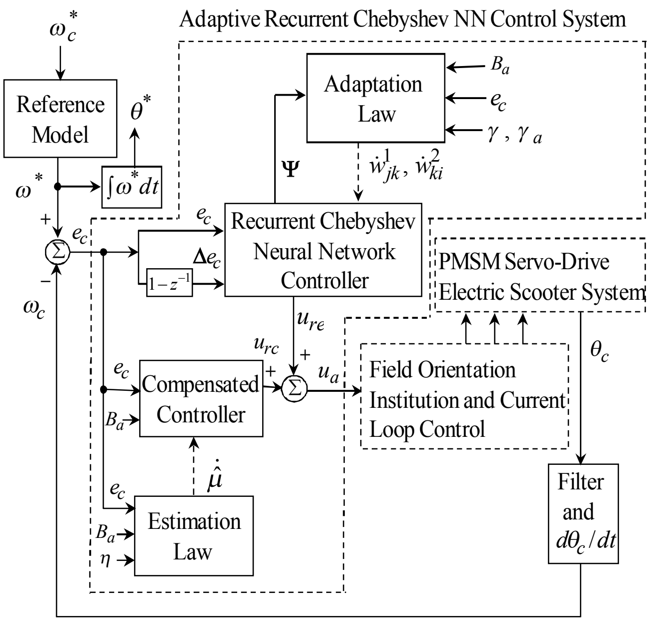

Fig. 2. Block diagram of adaptive recurrent Chebyshev NN control system.

The adaptive recurrent Chebyshev NN control system is composed of a recurrent Chebyshev NN controller and a compensated controller with estimation law. The control law is designed as

$$u_a = u_{re} + u_{rc} \tag{10}$$

where u_{re} is the recurrent Chebyshev NN control which is as the major tracking controller. It is used to imitate an ideal control law. The compensated control u_{rc} is designed to compensate the difference between the ideal control law and the recurrent Chebyshev NN control.

An error dynamic equation from (6) to (10) can be acquired as

$$\dot{e}_c = -k_1 e_c + [u_a^* - u_{re} - u_{rc}]B_a \tag{11}$$

The recurrent Chebyshev NN control and compensated control can be devised to conquer the mentioned drawback. The recurrent Chebyshev NN control raised to imitate the ideal control u_a^*. Then a compensated control posed to compensate the difference between ideal control u_a^* and the recurrent Chebyshev NN control u_{re} , and meanwhile compensate the lumped nonlinear external disturbances and the variation of parameters uncertainties.

3.1 Recurrent Chebyshev NN

Firstly, the architecture of the proposed three-layer recurrent Chebyshev NN is depicted in Fig. 3. It is composed of an input, a hidden and an output layers. The activation functions and signal actions of nodes in each layer of the recurrent Chebyshev NN can be described as follows:

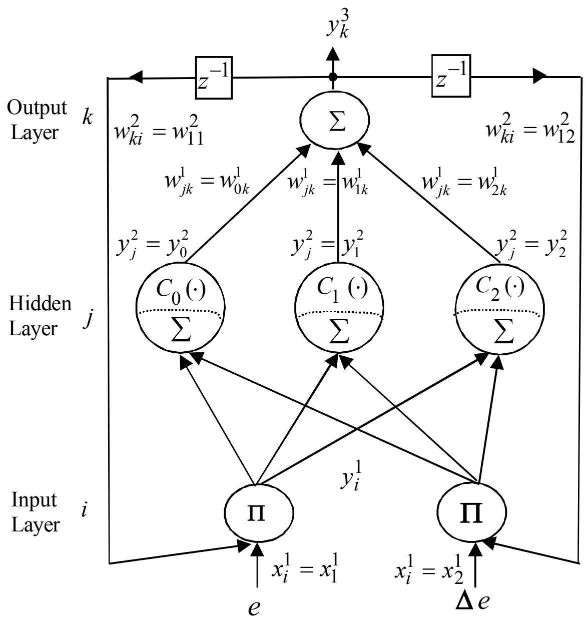

Fig. 3. Structure of the three-layer recurrent Chebyshev NN.

First layer: input layer

Each node i in this layer is indicated by using Π , which multiplies by each other between each other for input signals. Then outputs signals are the results of product. The input and the output for each node i in this layer are expressed as

$$nod_i^1 = x_i^1(N) w_{ki}^2 y_k^3(N-1),$$
$$y_i^1 = f_i^1(nod_i^1) = nod_i^1, \quad i = 1, 2 \text{ and } k = 1 \tag{12}$$

The $x_1^1 = \omega^* - \omega_c = e_c$ is the tracking error between the desired speed ω^* and the rotor speed ω_c . The $x_2^1 = e_c(1 - z^{-1}) = \Delta e_c$ is the tracking error change. The w_{ki}^2 is the recurrent weight between output layer and input layer. The N denotes the number of iterations. The y_k^3 is the output value of the output layer in the recurrent Chebyshev NN.

Second layer: hidden layer

The single node jth in this layer is labeled with $\sum$. The net input and the net output for node jth of the hidden layer are expressed as

$$nod_j^2 = \sum_{i=1}^{2} y_i^1,$$
$$y_j^2 = f_j^2(nod_j^2) = C_j(nod_j^2), \; j = 0, 1, 2 \tag{13}$$

Chebyshev polynomials (Namatame and Ueda, 1992; Lee and Jeng, 1998) are selected for activation function of the hidden layer. The first few Chebyshev polynomials are given by $C_0(x) = 1$, $C_1(x) = x$ and $C_2(x) = 2x^2 - 1$. The higher order Chebyshev polynomials may be generated by the recursive formula given by $C_{n+1}(x) = 2xC_n(x) - C_{n-1}(x)$.

Third layer: output layer

The single node kth in this layer is labeled with $\sum$. It computes the overall output as the summation of all input signals. The net input and the net output for node kth in this layer are expressed as

$$nod_k^3 = \sum_{j=0}^{2} w_{jk}^1 y_j^2,$$

$$y_k^3 = f_k^3(nod_k^3) = nod_k^3, \quad k=1 \tag{14}$$

where w_{jk}^1 is the connective weight between the hidden layer and the output layer; f_k^3 is the activation function, which is selected as a linear function; $x_j^3(N) = y_j^2(N)$ represents the jth input to the node of output layer. The output value of the recurrent Chebyshev NN can be represented as $y_k^3(N) = u_{re}$. Then the output value of the recurrent Chebyshev NN, u_{re}, can be denoted as

$$u_{re} = \mathbf{\Theta}^T \mathbf{\Psi} \tag{15}$$

in which $\mathbf{\Theta} = \begin{bmatrix} w_{01}^1 & w_{11}^1 & w_{21}^1 \end{bmatrix}^T$ is the adjustable weight parameters vector between the hidden layer and the output layer of the recurrent Chebyshev NN. $\mathbf{\Psi} = \begin{bmatrix} x_0^3 & x_1^3 & x_2^3 \end{bmatrix}^T$ is the inputs vector in the output layer of the recurrent Chebyshev NN, in which x_j^3 is determined by the selected Chebyshev polynomials.

3.2 Compensated Control with Estimation Law

Secondly, in order to evolve the remunerated control u_{rc}, a minimum affinity error σ is defined as

$$\sigma = u_a^* - u_{re}^* = u_a^* - (\mathbf{\Theta}^*)^T \mathbf{\Psi} \tag{16}$$

in which $u_{re}^* = (\mathbf{\Theta}^*)^T \mathbf{\Psi}$ is an ideal recurrent Chebyshev NN control law which is to reach of minimum affinity error σ between the ideal control law u_a^* and the ideal recurrent Chebyshev NN control law u_{re}^* ; $\mathbf{\Theta}^*$ is an ideal recurrent Chebyshev NN weight vector to reach of minimum affinity error. The recurrent Chebyshev NN control u_{re} raised to approximate the ideal recurrent Chebyshev NN control law u_{re}^* . It is assumed that absolute value of σ is less than a small positive constant μ , i.e., $|\sigma| < \mu$. The compensated controller u_{rc} with estimation law is developed to compensate between the ideal control law u_a^* and the ideal recurrent Chebyshev NN control law u_{re}^* , and meanwhile compensate the lumped nonlinear external disturbances and the variation of parameters uncertainty. Furthermore, the adaption law is also developed to online tuning parameters of the recurrent Chebyshev NN. Hence, the error dynamic equation by means of (11) can be rewritten as

$$\begin{aligned}
\dot{e}_c &= -k_1 e_c + [(u_a^* - u_{re}) - u_{rc}]B_a \\
&= -k_1 e_c + [(u_a^* - u_{re}^* + u_{re}^* - u_{re}) - u_{rc}]B_a \\
&= -k_1 e_c + [(u_a^* - u_{re}^*) + (\mathbf{\Theta}^*)^T \mathbf{\Psi} - (\mathbf{\Theta})^T \mathbf{\Psi}) - u_{rc}]B_a \\
&= -k_1 e_c + [\sigma + (\mathbf{\Theta}^* - \mathbf{\Theta})^T \mathbf{\Psi} - u_{rc}]B_a
\end{aligned} \tag{17}$$

Then, the Lyapunov function is selected as

$$v_1(t) = e_c^2/2 + (\mathbf{\Theta}^* - \mathbf{\Theta})^T (\mathbf{\Theta}^* - \mathbf{\Theta})/(2\gamma) + \tilde{\mu}^2/(2\eta) \tag{18}$$

in which γ is a learning rate of connective weight; $\tilde{\mu} = \hat{\mu} - \mu$ is the bound estimated error; η is an adaptation gain. Differentiating the Lyapunov function with respect to t and using (17), then (18) can be rewritten as

$$\begin{aligned}
&\dot{v}_1(t) = \dot{e}_c e_c - (\mathbf{\Theta}^* - \mathbf{\Theta})^T \dot{\mathbf{\Theta}}/\gamma + \tilde{\mu}\dot{\hat{\mu}}/\eta \\
&= \{-k_1 e_c + [\sigma - u_{rc}]B_a\} e_c + \tilde{\mu}\dot{\hat{\mu}}/\eta \\
&+ (\mathbf{\Theta}^* - \mathbf{\Theta})^T \mathbf{\Psi} B_a e_c - (\mathbf{\Theta}^* - \mathbf{\Theta})^T \dot{\mathbf{\Theta}}/\gamma
\end{aligned} \tag{19}$$

In order to $\dot{v}_1 \le 0$, the adaptation law $\dot{\mathbf{\Theta}}$, the compensated controller u_{rc} with estimation law can be designed as follows

$$\dot{\mathbf{\Theta}} = \gamma \mathbf{\Psi} B_a e_c \tag{20}$$

$$u_{rc} = \hat{\mu}\,\mathrm{sgn}(B_a e_c) \tag{21}$$

$$\dot{\hat{\mu}} = \eta |B_a e_c| \tag{22}$$

In order to avoid chattering phenomenon of sliding mode, the sign function $\mathrm{sgn}(B_a e_c)$ can be replaced by the equation $B_a e_c / (|B_a e_c| + \rho)$, where $\rho = \begin{cases} \rho_0, & |B_a e_c| < \varepsilon \\ 0, & |B_a e_c| \ge \varepsilon \end{cases}$, ρ_0 and ε are positive constants. Substituting (20) into (19), then (19) can be represented as

$$\dot{v}_1(t) = -k_1 e_c^2 + \{\sigma - u_{rc}\} B_a e_c + \tilde{\mu}\dot{\hat{\mu}}/\eta \tag{23}$$

Substituting (21) and (22) into (23), then (23) can be obtained as

$$\begin{aligned}
\dot{v}_1(t) &= -k_1 e_c^2 + \{\sigma - \hat{\mu}\,\mathrm{sgn}(B_a e)\} B_a e_c + (\hat{\mu} - \mu)(\eta |B_a e_c|)/\eta \\
&\le -k_1 e_c^2 + \{|\sigma| - \hat{\mu}\} |B_a e_c| + (\hat{\mu} - \mu) |B_a e_c| \\
&= -k_1 e_c^2 + \{|\sigma| - \mu\} |B_a e_c| \\
&\le -k_1 e_c^2 \\
&\le 0
\end{aligned} \tag{24}$$

From (24), the $\dot{v}_1(t)$ is a negative semi-definite function, i.e., $v_1(t) \le v_1(0)$. It implies that e_c and $(\mathbf{\Theta}^* - \mathbf{\Theta})$ be bounded. For the sake of proof of the proposed adaptive recurrent Chebyshev NN control system to be asymptotically stable, the function is defined as

$$\phi(t) = -\dot{v}_1(t) = k_1 e_c^2 \tag{25}$$

Integrating (25) with respect to t , then

$$\int_0^t \phi(\tau)d\tau = \int_0^t [-\dot{v}_1(t)]dt = v_1(0) - v_1(t) \quad (26)$$

Owing to $v_1(0)$ is bounded, and $v_1(t)$ is a non-increasing and bounded function, the

$$\lim_{t\to\infty} \int_0^t \phi(\tau)d\tau < \infty \quad (27)$$

Differentiating (25) with respect to *t* gives

$$\dot{\phi}(t) = 2k_1 e_c \dot{e}_c \quad (28)$$

Owing to all the variables in the right side of (17) are bounded. It implies that $\dot{e}_c$ is also bounded. Then, $\phi(t)$ is a uniformly continuous function (Astrom and Wittenmark, 1995; Slotine and Li, 1991). It is denoted that $\lim_{t\to\infty}\phi(t) = 0$ by using Barbalat's lemma (Astrom and Wittenmark, 1995; Slotine and Li, 1991), i.e., $e_c(t) \to 0$ as $t \to \infty$. Therefore, the adaptive recurrent Chebyshev NN control system is asymptotically stable. Moreover, the tracking error $e_c(t)$ of the system will converge to zero.

3.3 Convergence Analyses

The adaptation law shown in (20) calls for a proper choice of the learning rate. For a small value of learning rate, the convergence of controller parameter can be guaranteed but the convergent speed is very slow. On the other hand, if the learning-rate is too large, the parameter convergence may become more unstable. According to Lyapunov stability theorem and the gradient descent method, an online parameter tuning methodology of the recurrent Chebyshev NN can be derived and tuned effectively. The parameters of adaptation law $\dot{\Theta}$ can be computed by the gradient descent method and the chain rule. First, the adaptation law $\dot{\Theta}$ shown in (20) can be rewritten as

$$\dot{w}_{jk}^1 = \gamma\, x_j^3 B_a e_c, \quad j = 0, 1, 2 \text{ and } k = 1 \quad (29)$$

The central part of the tuning algorithm for the recurrent Chebyshev NN concerns how to obtain recursively a gradient vector in which each element in the tuning algorithm is defined as the derivative of an energy function with respect to a parameter of the network. This is done by means of the chain rule, because the gradient vector is calculated in the direction opposite to the flow of the output of each node. In order to describe the online tuning algorithm of the recurrent Chebyshev NN, a cost function is defined as

$$V_1 = e_c^2 / 2 \quad (30)$$

According to the gradient descent method, the adaptation law of the weight between the hidden layer and the output layer also can be represented as

$$\begin{aligned}\dot{w}_{jk}^1 &= -\gamma \frac{\partial V_1}{\partial w_{jk}^1} \\ &= -\gamma \frac{\partial V_1}{\partial u_{re}} \frac{\partial u_{re}}{\partial y_k^3} \frac{\partial y_k^3}{\partial nod_k^3} \frac{\partial nod_k^3}{\partial w_{jk}^1} = -\gamma \frac{\partial V_1}{\partial y_k^3} x_j^3 \end{aligned} \quad (31)$$

Comparing (29) with (31), yields $\partial V_1 / \partial y_k^3 = -B_a e_c$.

The adaptation law of recurrent weight w_{ki}^2 using the gradient descent method can be updated as

$$\begin{aligned}\dot{w}_{ki}^2 &= -\gamma_a \frac{\partial V_1}{\partial u_{re}} \frac{\partial u_{re}}{\partial y_k^3} \frac{\partial y_k^3}{\partial y_j^2} \frac{\partial y_j^2}{\partial nod_j^2} \frac{\partial nod_j^2}{\partial y_i^1} \frac{\partial y_i^1}{\partial nod_i^1} \frac{\partial nod_i^1}{\partial w_{ki}^2} \\ &= \gamma_a B_a\, e_c w_{jk}^1 C_j(\cdot) x_i^1(N) y_k^3(N-1)\end{aligned} \quad (32)$$

in which γ_a is an adaptation gain.

4. EXPERIMENTAL RESULTS

The whole system of the DSP-based control system for a PMSM servo-drive electric scooter system is shown in Fig. 1. The control algorithm was executed by a TMS320C32 DSP control system including 4 channels of D/A converter, 8 channels of programmable PWM and an encoder interface circuit. The methodologies proposed for the real-time control implementation in the DSP control system are composed of the main program and the interrupt service routine (ISR) as shown in Fig. 4. In the main program, parameters and input/output (I/O) initialization are processed first. Then, the interrupt interval for the ISR is set. After enabling the interrupt, the main program is used to monitor control data. The ISR with 2 *ms* sampling interval is used for reading the rotor position of the PMSM servo-driven electric scooter from encoder circuit and three-phase currents from A/D converter, calculating rotor position and speed, executing lookup table and coordinate translation, executing PID current control, executing the adaptive recurrent Chebyshev NN control system, and outputting three-phase current commands via D/A converter to sinusoidal PWM circuit for switching three-sets IGBT power modules inverter through interlock and isolated circuits. The voltage source inverter with 3 sets of IGBT power modules is executed by current-controlled sinusoidal PWM circuit with a switching frequency of 15 *k*Hz by using triangular carrier wave. The specification of the used PMSM is 3-phase 48 V, 750 W, 3600 *rpm*. The parameters of the PMSM are given as $\bar{J}_r = 62.15 \times 10^{-3}\, Nms$, $\bar{B}_r = 6.18 \times 10^{-3}\, Nms/rad$, $R_r = 2.5\Omega$, $L_{dr} = L_{qr} = 6.53\, mH$, $k_r = 0.86\, Nm/A$ by means of open circuit test, short test, rotor block test, loading test.

The adaptive recurrent Chebyshev NN control system control performance is compared with baseline controller: the PI controller. Owing to inherent uncertainty in electric scooter and output current limitation of battery power capacity, a PMSM can only operate at 251.2 *rad/s* due to high speed perturbation. The PI control method and the adaptive recurrent Chebyshev NN control method are tested via two cases in the experimentation here, one being the125.6 *rad/s* case, another being 251.2 *rad/s* case. Because the electric scooter driven by PMSM has highly nonlinear and time-varying characteristics, all gains of the PI controller , which is listed as $k_{ps} = 16$ and $k_{is} = 4$ for the speed tracking at 125.6 *rad/s* case by experimental result, are obtained by try and error method in order to achieve good transient and steady-state control performance.

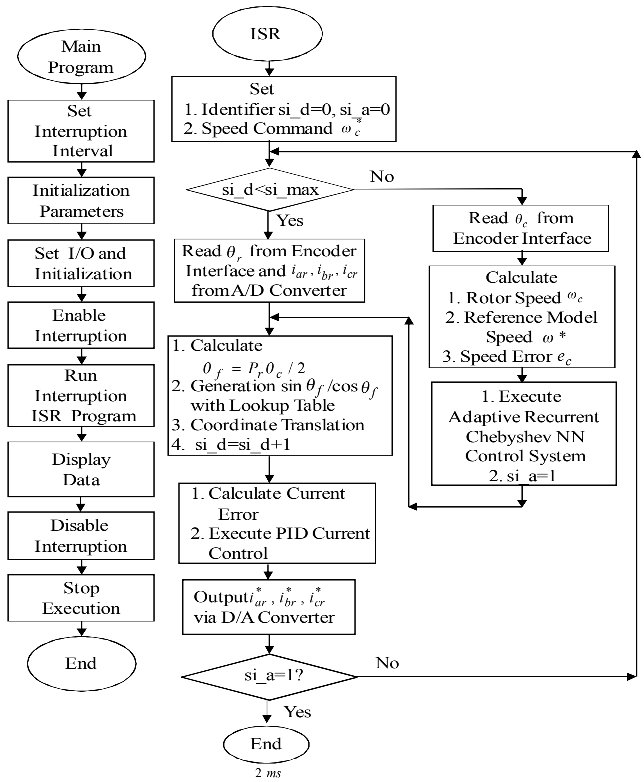

Fig. 4. Flowchart of the executing program by using the DSP control system.

The speed tracking response of the command rotor speed ω_c^*, the desired command rotor speed ω^* and the measured rotor speed ω_c for a PMSM servo-drive electric scooter using the PI controller at 125.6 *rad/s* case is shown in Fig. 5. The zoom error of speed response for a PMSM servo-drive electric scooter using the PI controller at 125.6 *rad/s* is shown in Fig. 6. The position tracking response of the desired command rotor position θ^* and the measured rotor position θ_c for a PMSM servo-drive electric scooter using the PI controller at 125.6 *rad/s* case is shown in Fig. 7. The current tracking response of the command current i_{ar}^* and measured current i_{ar} in phase *a* for a PMSM servo-drive electric scooter using the PI controller at 125.6 *rad/s* case is shown in Fig. 8.

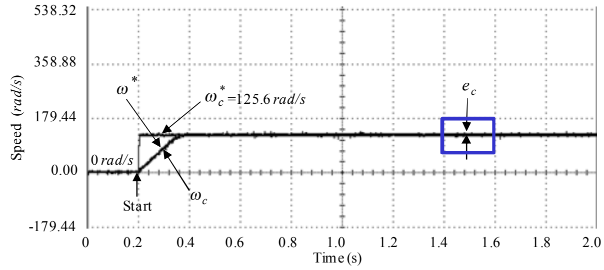

Fig. 5. Speed tracking response using the PI controller at 125.6 *rad/s* case.

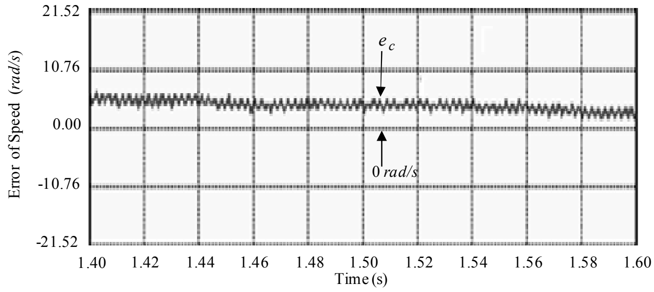

Fig. 6. Zoom error of speed response using the PI controller at 125.6 *rad/s* case.

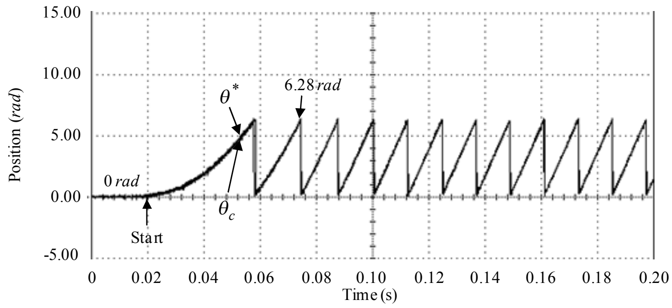

Fig. 7. Position tracking response using the PI controller at 125.6 *rad/s* case.

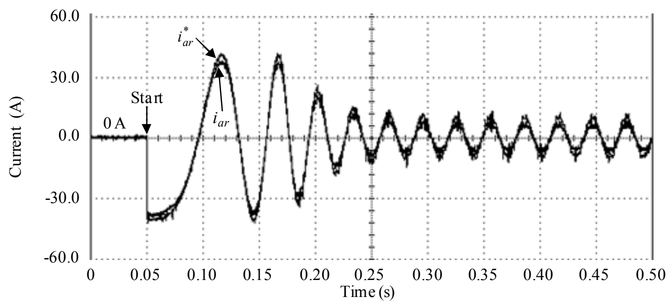

Fig. 8. Current tracking response using the PI controller at 125.6 *rad/s* case.

The speed tracking response of the command rotor speed ω_c^*, the desired command rotor speed ω^* and the measured rotor speed ω_c for a PMSM servo-drive electric scooter using the PI controller at 251.2 *rad/s* case is shown in Fig. 9. The zoom error of speed response for a PMSM servo-drive electric scooter using the PI controller at 251.2 *rad/s* is shown in Fig. 10. The position tracking response of the desired command rotor position θ^* and the measured rotor position θ_c for a PMSM servo-drive electric scooter using the PI controller at 251.2 *rad/s* case is shown in Fig. 11. The current tracking response of the command current i_{ar}^* and measured current i_{ar} in phase *a* for a PMSM servo-drive electric scooter using the PI controller at 251.2 *rad/s* case is shown in Fig. 12.

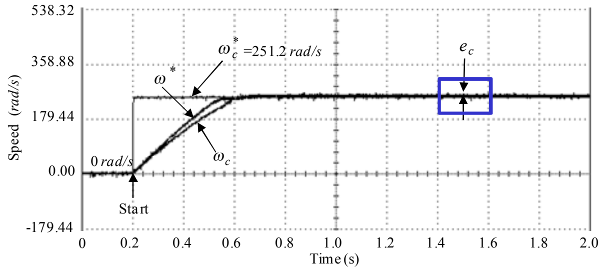

Fig. 9. Speed tracking response using the PI controller at 251.2 *rad/s* case.

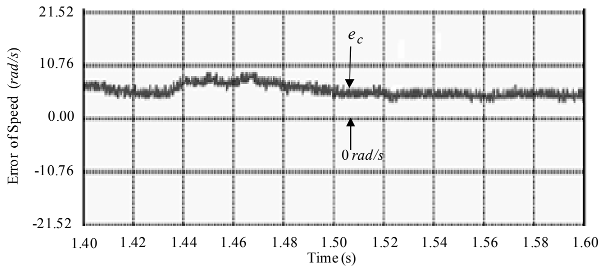

Fig. 10. Zoom error of speed response using the PI controller at 251.2 *rad/s* case.

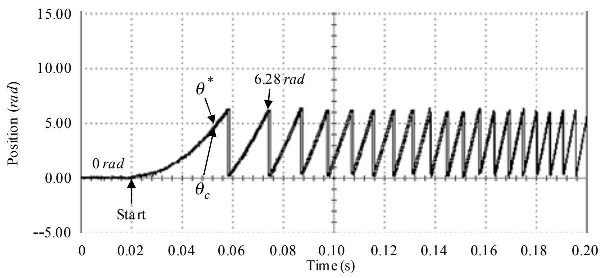

Fig. 11. Position tracking response using the PI controller at 251.2 *rad/s* case.

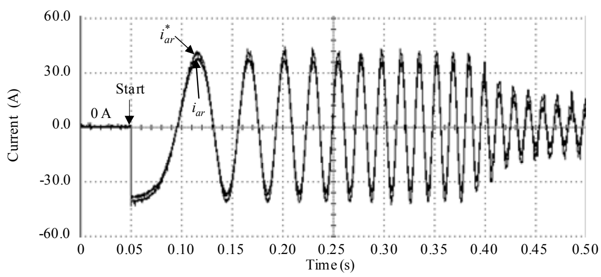

Fig. 12. Current tracking response using the PI controller at 251.2 *rad/s* case.

Since the low speed operation is the same as the nominal case due to smaller the lumped external disturbances with parameter variations, the speed and position tracking responses using the

PI controller shown in Figs. 5 and 7 have better tracking performances. But the zoom errors of speed using the PI controller shown in Figs. 6 and 10 are larger and slower convergence. The degenerate speed and position tracking responses using the PI controller shown in Figs. 9 and 11 resulted owing to the occurrence of the larger external disturbances and parameter variations. In addition, the current tracking responses using the PI controller shown in Figs. 8, and 12 resulted great chattering due to action on electric scooter system with highly nonlinear disturbances such as nonlinear friction between primary pulley and second pulley. From the experimental results, sluggish speed tracking responses using the PI controller for a PMSM servo-drive electric scooter are obtained owing to the weak robustness of the linear controller without online adjustment mechanism.

The control gains of the proposed adaptive recurrent Chebyshev NN control system are selected as $\gamma = 0.05$, $\gamma_a = 0.02$ and $\eta = 0.2$ in order to achieve the best transient control performance in experimentation considering the requirement of stability. The parameter adjustment process remains continually active for the duration of the experimentation. The experimental results of the adaptive recurrent Chebyshev NN control system for a PMSM servo-drive electric scooter at 125.6*rad/s* case and 251.2*rad/s* case are shown in Figs. 13-20. The speed tracking response of the command rotor speed ω_c^*, the desired command rotor speed ω^* and the measured rotor speed ω_c for a PMSM servo-drive electric scooter using the adaptive recurrent Chebyshev NN control system at 125.6 *rad/s* case is shown in Fig. 13. The zoom error of speed response for a PMSM servo-drive electric scooter using the adaptive recurrent Chebyshev NN control system at 125.6 *rad/s* is shown in Fig. 14. The position tracking response of the desired command rotor position θ^* and the measured rotor position θ_c for a PMSM servo-drive electric scooter using the adaptive recurrent Chebyshev NN control system at 125.6 *rad/s* case is shown in Fig. 15. The current tracking response of the command current i_{ar}^* and measured current i_{ar} in phase *a* for a PMSM servo-drive electric scooter using the adaptive recurrent Chebyshev NN control system at 125.6 *rad/s* case is shown in Fig. 16.

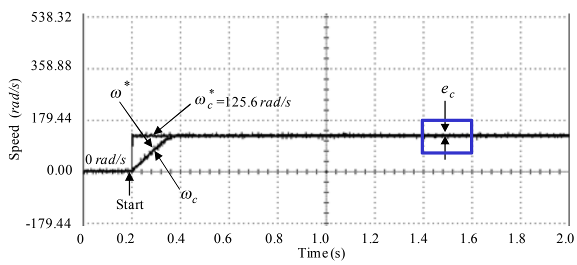

Fig. 13. Speed tracking response using the adaptive recurrent Chebyshev NN control system at 125.6 *rad/s* case.

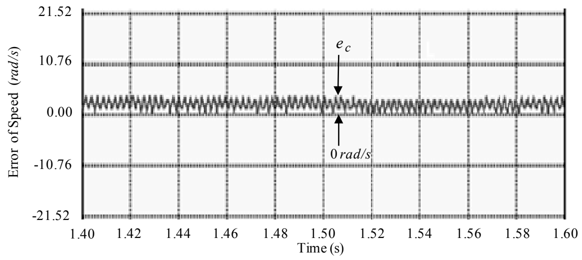

Fig. 14. Zoom error of speed response using the adaptive recurrent Chebyshev NN control system at 125.6 *rad/s* case.

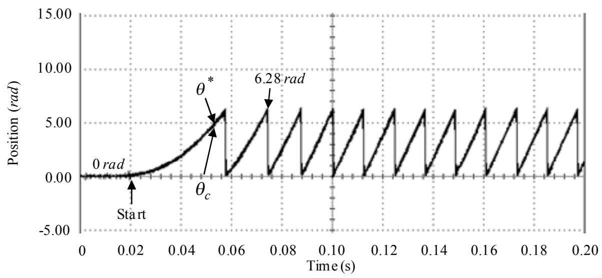

Fig. 15. Position tracking response using the adaptive recurrent Chebyshev NN control system at 125.6 *rad/s* case.

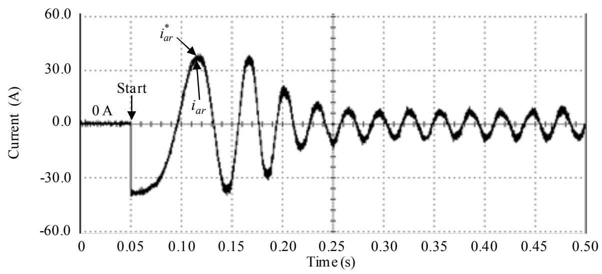

Fig. 16. Current tracking response using the adaptive recurrent Chebyshev NN control system at 125.6 *rad/s* case.

The speed tracking response of the command rotor speed ω_c^*, the desired command rotor speed ω^* and the measured rotor speed ω_c for a PMSM servo-drive electric scooter using the adaptive recurrent Chebyshev NN control system at 251.2 *rad/s* case is shown in Fig. 17. The zoom error of speed response for a PMSM servo-drive electric scooter using the adaptive recurrent Chebyshev NN control system at 251.2 *rad/s* is shown in Fig. 18. The position tracking response of the desired command rotor position θ^* and the measured rotor position θ_c for a PMSM servo-drive electric scooter using the adaptive recurrent Chebyshev NN control system at 251.2 *rad/s* case is shown in Fig. 19. The current tracking response of the command current i_{ar}^* and measured current i_{ar} in phase *a* for a PMSM servo-drive electric scooter using the adaptive recurrent Chebyshev NN control system at 251.2 *rad/s* case is shown in Fig. 20.

Since the low speed operation is the same as the nominal case due to smaller the lumped external disturbances and parameters variations, speed and position tracking responses for two control systems shown in Figs. 5, 7, 13 and 15 have better tracking performances. Due to online adjusted ability of the adaptive recurrent Chebyshev NN control system, zoom errors of tracking speed using the PI controller shown in Figs. 6 and 10 have larger error and slower convergence than the adaptive recurrent Chebyshev NN control system shown in Figs. 14 and 18. Meanwhile, the speed and position tracking responses using the adaptive recurrent Chebyshev NN control system shown in Figs. 17 and 19 have better tracking performances than using the PI controller shown in Figs. 9 and 11 under the occurrence of the larger external disturbances and parameter variations. In addition, current tracking responses by means of the PI controller shown in Figs. 8 and 12 have larger chattering phenomena than the adaptive recurrent Chebyshev NN control system shown in Figs. 16 and 20. That is due to online adjustment ability of the adaptive recurrent Chebyshev NN to cope with high frequency unmodeled dynamics of the controlled plant. The zoom errors of tracking speed by means of the PI controller and the adaptive recurrent Chebyshev NN control system at 251.2 *rad/s* are shown in Figs. 10 and 18, respectively. However, owing to online adaptive mechanism of the recurrent Chebyshev NN and action of the compensated controller, accurate tracking control performance of the PMSM servo-drive electric scooter can be obtained. Additionally, the small chattering phenomena of the currents in phase *a* shown in Figs. 16 and 20 are induced by online adjustment of the recurrent Chebyshev NN to cope with highly nonlinear dynamics of system. Furthermore, the adaptive recurrent Chebyshev NN control system has faster convergence than the PI controller as comparison Fig. 10 with Fig. 18 due to online adaptive mechanism action of recurrent Chebyshev NN. These experimental results show that the adaptive recurrent Chebyshev NN control system has better performance than the PI controller for a PMSM servo-drive electric scooter.

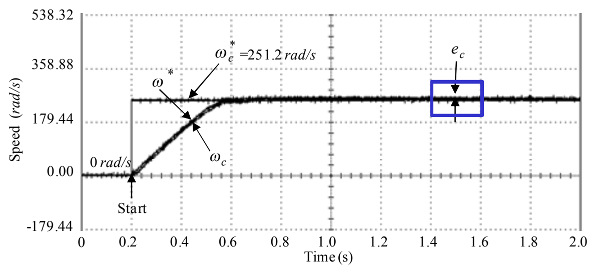

Fig. 17. Speed tracking response using the adaptive recurrent Chebyshev NN control system at 251.2 *rad/s* case.

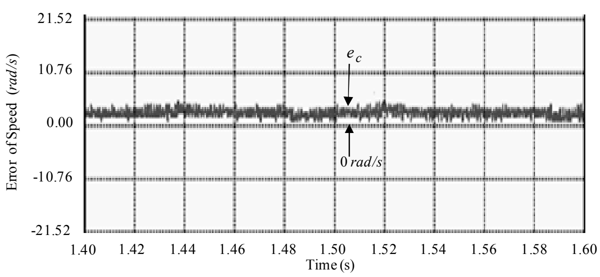

Fig. 18. Zoom error of speed response using the adaptive recurrent Chebyshev NN control system at 251.2 *rad/s* case.

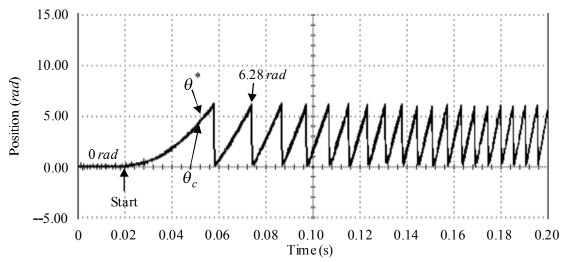

Fig. 19. Position tracking response using the adaptive recurrent Chebyshev NN control system at 251.2 *rad/s* case.

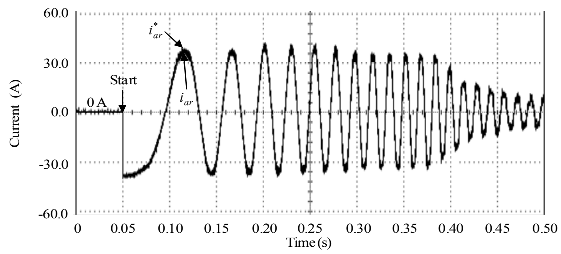

Fig. 20. Current tracking response using the adaptive recurrent Chebyshev NN control system at 251.2 *rad/s* case.

Finally, the measurement of load regulation under step disturbance torque is tested. The PI control and the adaptive recurrent Chebyshev NN control system are tested under $T_l = 2\ Nm$ load torque disturbance with adding load and shedding load. The experimental results of the measured rotor speed responses and measured current in phase *a* using the PI controller under $T_l = 2\ Nm$ load torque disturbance with adding load and shedding load at 251.2 *rad/s* is shown in Fig. 21. The experimental results of the measured speed response and measured current in phase *a* using the adaptive recurrent Chebyshev NN control system under $T_l = 2\ Nm$ load torque disturbance with adding load and shedding load at 251.2 *rad/s* is shown in Fig. 23. The zoom errors of speed of the PI controller and the adaptive recurrent Chebyshev NN control system under $T_l = 2\ Nm$ load torque disturbance with adding load and shedding load at 251.2 *rad/s* are shown in Figs. 22, and 24, respectively.

From the experimental results, the degenerated response under the variation of rotor inertia and load torque disturbance is much improved by means of the adaptive recurrent Chebyshev NN control system. From experimental results, transient response of the adaptive recurrent Chebyshev NN control system is better than the PI controller at load regulation.

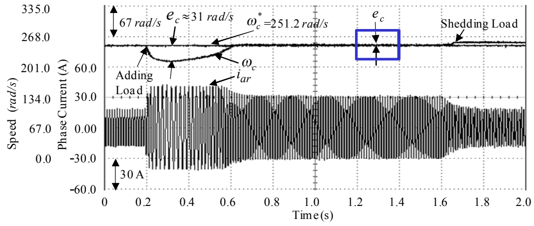

Fig. 21. Load regulation response using the PI controller under $T_l = 2\,Nm$ load torque disturbance.

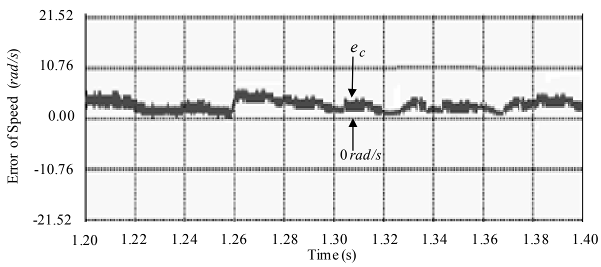

Fig. 22. Zoom error of speed response using the PI controller under $T_l = 2\,Nm$ load torque disturbance.

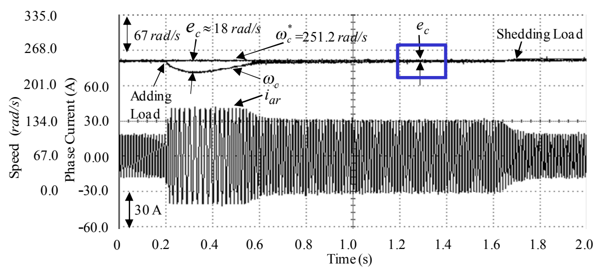

Fig. 23. Load regulation response using the adaptive recurrent Chebyshev NN control system under $T_l = 2\,Nm$ load torque disturbance.

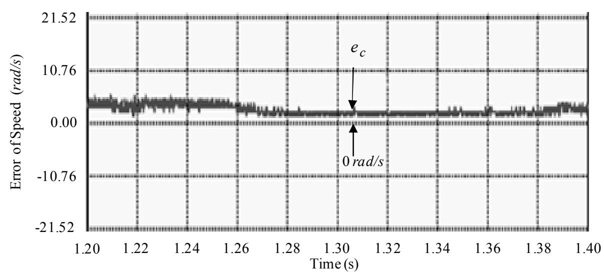

Fig. 24. Zoom error of speed response using the adaptive recurrent Chebyshev NN control system under $T_l = 2\,Nm$ load torque disturbance.

5. CONCLUSION

A PMSM servo-drive electric scooter system controlled by the adaptive recurrent Chebyshev NN control system with online parameters adjustment and fast convergence has been successfully developed in this study.

Firstly, the dynamic models of the PMSM servo-drive electric scooter system were derived. Because the electric scooter is a nonlinear and time-varying system, sluggish speed tracking is obtained for the PI controlled PMSM servo-drive electric scooter owing to the weak robustness of the linear controller. Therefore, the PMSM servo-drive electric scooter controlled by the adaptive recurrent Chebyshev NN control system is developed in order to raise robustness under the occurrence of the variation of rotor inertia and load torque disturbance.

Secondly, the online parameter tuning methodology of the recurrent Chebyshev NN and the estimation law of the compensated controller are derived by using the Lyapunov stability theorem.

In addition, the adaptive recurrent Chebyshev NN control system has fast convergence ability and good online learning capability in order to be able to fast capture the system's nonlinear and time-varying behaviors.

Moreover, the compensated control with estimation law posed to compensate the difference between ideal control and the recurrent Chebyshev NN control, and meanwhile compensate the lumped nonlinear external disturbances and the variation of parameters uncertainty.

Finally, the control performance of the proposed adaptive recurrent Chebyshev NN control system is more suitable than the PI controller for the PMSM servo-drive electric scooter system from experimental results.

REFERENCES

Astrom, K.J., and Wittenmark, B. (1995) *Adaptive Control*, Addison-Wesley, New York.

Battiti, R. (1992) First- and second-order methods for learning: Between steepest descent and Newton's method, *Neural Computation*, (4), 141-166.

Brdys, M.A. and Kulawski, G.J. (1999) Dynamic neural controllers for induction motor, *Transactins on Neural Networks*, (10), 340-355.

Charalambous, C. (1992) Conjugate gradient algorithm for efficient training of artificial neural networks, *Proceedings Institute Electrical Engineering Part-G*, (139), 301-310.

Chow, T.W.S., and Fang, Y. (1998) A recurrent neural-network-based real-time learning control strategy applying to nonlinear systems with unknown dynamics, *IEEE Transactins on Industrial Electronics*, (45), 151-161.

Ciliz, M.K. (2005) Adaptive control of robot manipulators with neural network based compensation of frictional uncertainties, *Robotica*, (23), 159–167.

Grino, R., Cembrano, G., and Torras, C. (2000) Nonlinear system identification using additive dynamic neural networks – two on-line approaches, *IEEE Transactins on Circuits and Systems Part-I*, (47), 150-165.

Hagan, M.T., Menhaj, M.B. (1994) Training feedforward networks with Marquardt algorithm, *IEEE Transactins on Neural Networks*, (5), 989-993.

Haykin, S. (1994) *Neural networks,* Maxwell Macmillan, Ottawa, Canada.

Lee, T.T., and Jeng, J.T. (1998) The Chebyshev polynomial-based unified model neural networks for functional approximation, *IEEE Transactins on System, Man and Cybernetics Part-B*, (28), 925-935.

Leonhard, W. (1996) *Control of Electrical Drives*, Springer-Verlag, Berlin.

Li, X.D., J. K. L. Ho, J.K.L, and Chow, T.W.S. (2005) Approximation of dynamical time-variant systems by continuous-time recurrent neural networks, *IEEE Transactins on Circuits and Systems Part-II*, (52), 656-660.

Lin, C.H., Chiang, P.H., Tseng, C.S., Lin, Y.L., and Lee, M.Y. (2010) Hybrid recurrent fuzzy neural network control for permanent magnet synchronous motor applied in electric scooter, *International Power Electronics Conference*, Sapporo, 1371-1376.

Lin, C.H., and Lin, C.P. (2012) The hybrid RFNN control for a PMSM drive system using rotor flux estimator, *International Journal of Power Electronics*, (4), 33-48.

Lin, C.H., Lin, C.P. (2013) Hybrid modified Elman NN controller design on permanent magnet synchronous motor driven electric scooter, *Transactions of the Canadian Society for Mechanical Engineering*, (37), 1127-1145.

Lin, C.H. (2014) A novel hybrid recurrent wavelet neural network control of PMSM servo-drive system for electric scooter, *Turkish Journal of Electrical Engineering and Computer Sciences*, (22), 1056-1075.

Lin, F.J. (1997) Real-time IP position controller design with torque feedforward control for PM synchronous motor, *IEEE Transactins on Industrial Electronics*, (4), 398-407.

Lu, C.H., and Tsai, C.C. (2008) Adaptive predictive control with recurrent neural network for industrial processes: an application to temperature control of a variable-frequency oil-cooling machine, *IEEE Transactins on Industrial Electronics*, (55), 1366-1375.

Madyastha, R.K., and Aazhang, B. (1994) An algorithm for training multilayer perceptrons for data classification and function interpolation, *IEEE Transactins on Circuits and Systems Part-I*, (41), 866-875.

Moller, M.F. (1993) A scaled conjugate gradient algorithm for fast supervised learning, *Neural Networks*, (6), 525-533.

Namatame, A., and Ueda, N. (1992) Pattern classification with Chebyshev neural networks, *International Journal of Neural Networks*, (3), 23-31.

Novotny, D. W., and Lipo, T.A. (1996) *Vector Control and Dynamics of AC Drives*, Oxford University Press, New York.

Patino, H.D., Carelli, R., and Kuchen, B.R. (2002) Neural networks for advanced control of robot manipulators, *IEEE Transactions on Neural Networks,* (13), 343–354.

Payam, A.F., Hashemnia, M.N., and Faiz, J. (2011) Robust DTC control of doubly-fed induction machines based on input-output feedback linearization using recurrent neural networks, *Journal of Power Electronics*, (11), 719-725.

Sastry, P.S., Santharam, G., and Unnikrishnan, K.P. (1994) Memory neural networks for identification and control of dynamical systems, *IEEE Transactions on Neural Networks*, (5), 306-319.

Sefriti, S., Boumhidi, J., Naoual, R., and Boumhidi, I. (2012) Adaptive neural network sliding mode control for electrically-driven robot manipulators, *Journal of Control Engineering and Applied Informatics*, (14), 27-32.

Slotine, J.J.E., and Li. W. (1991) *Applied Nonlinear Control*, Prentice-Hall, Englewood Cliffs, New Jersey.

Sun, F.C., Sun, Z.Q., Zhang, R.J., and Chen, Y.B. (2000) Neural adaptive tracking controller for robot manipulators with unknown dynamics, *IEE Proceedings Control Theory and Application,* (147), 366-370.

Sun, T., Pei, H., Pan, Y., Zhou, H., and Zhang, C. (2011) Neural network-based sliding mode adaptive control for robot manipulators, *Neurocomputing*, (74), 2377–2384.